Cracking Urban Mobility

H. A. Carmona,[1] A. W. T. de Noronha,[1] A. A. Moreira,[1] N. A. M. Araujo,[1,2,3] and J. S. Andrade Jr.[1,*]

[1] *Departamento de Física, Universidade Federal do Ceará, 60451-970 Fortaleza, Ceará, Brazil*
[2] *Departamento de Física, Faculdade de Ciências, Universidade de Lisboa, 1749-016 Lisboa, Portugal*
[3] *Centro de Física Teórica e Computacional, Universidade de Lisboa, 1749-016 Lisboa, Portugal*

Assessing the resilience of a road network is instrumental to improve existing infrastructures and design new ones. Here we apply the optimal path crack model (OPC) to investigate the mobility of road networks and propose a new proxy for resilience of urban mobility. In contrast to static approaches, the OPC accounts for the dynamics of re-routing as a response to traffic jams. Precisely, one simulates a sequence of failures (cracks) at the most vulnerable segments of the optimal origin-destination paths that are capable to collapse the system. Our results with synthetic and real road networks reveal that their levels of disorder, fractions of unidirectional segments and spatial correlations can drastically affect the vulnerability to traffic congestion. By applying the OPC to downtown Boston and Manhattan, we found that Boston is significantly more vulnerable than Manhattan. This is compatible with the fact that Boston heads the list of American metropolitan areas with the highest average time waste in traffic. Moreover, our analysis discloses that the origin of this difference comes from the intrinsic spatial correlations of each road network. Finally, we argue that, due to their global influence, the most important cracks identified with OPC can be used to pinpoint potential small rerouting and structural changes in road networks that are capable to substantially improve urban mobility.

Traffic congestion is part of the daily life in a metropolitan region. In the top 20 cities in the US, it is estimated that the average daily commuter wastes more than 85 hours/year in traffic congestion [1]. Boston heads this list with a 160+ hours/year average delay. The numbers are even worst in cities like Moscow, London, Bogota, or Mexico City, where the average time wasted per year exceeds 200 hours. This inefficiency not only impacts on life quality and the environment, but it also compromises economic growth. A recent study using data from 88 US metropolitan areas suggests that a seemingly harmless average delay of 4.5 minutes for each one-way auto commute in a city is enough to slow down job growth [2].

To proper assess urban mobility, one needs to account for the impact of road congestion in global traffic [3–7]. Li *et al.* [8] proposed to apply Percolation Theory to evaluate how global connectivity is lost when vulnerable roads are congested. Their static analysis for different hours of the day gives insight into normal and rush-hour traffic and helped identifying vulnerable roads [4, 9–11]. However, in reality, users are actively evaluating their routes and taking alternative paths to avoid traffic jams [12–14]. Thus, the probability that a road gets congested depends, not only on its average level of traffic, but also on the likelihood that users take it in their route [15, 16].

Without central planning, travellers usually choose the route that minimizes their travelling time. However, when a road segment gets congested, a new optimal route needs to be found. The optimal path crack model (OPC) was introduced as a general framework to study the resilience of a network infrastructure to a sequence of optimal path failures [17, 18]. The OPC is described as follows. Let us consider a square lattice of size L with periodic boundary conditions in the horizontal direction and fixed boundary conditions at the top and bottom. To each link, a travelling time t is randomly assigned according to a given probability distribution $P(t)$, with $t > 0$. Using Dijkstra's algorithm [19], the first optimal path is identified which minimizes the total travelling time between the bottom and the top of the lattice. We then search and remove the most vulnerable link along this path, defined as the one with the highest travelling time. The next optimal path is identified, which cannot contain the removed link, and its vulnerable link is also removed. We proceed iteratively until the lattice is disrupted and no more paths can be found. The OPC is then the set of all removed links. In the limit of strong disorder, all cracks are located on a single self-similar connected line of fractal dimension equal to 1.22 [17]. As a matter of fact, this exponent value is statistically identical to the fractal dimension previously found for the optimal path line under strong disorder [20–23], "strands" in Invasion Percolation [20, 21], paths on Minimum Spanning Trees [24], and watersheds on uncorrelated landscapes [18]. In the case of weak disorder, the cracks spread all over the entire network before global connectivity is lost, so that the total number of removed links scales as $N_r \sim L^d$, where d is the topological dimension of the lattice [17].

So far, all studies of OPC considered undirected networks. However, traffic networks have a non-negligible fraction of one-way roads. For example, in Manhattan and Boston about half of the roads are unidirectional. Here we first perform simulations on square lattices in which the links are assigned to be unidirectional with probability p and bidirectional with probability $(1-p)$. For $p = 0$ we recover the OPC of a fully bidirectional

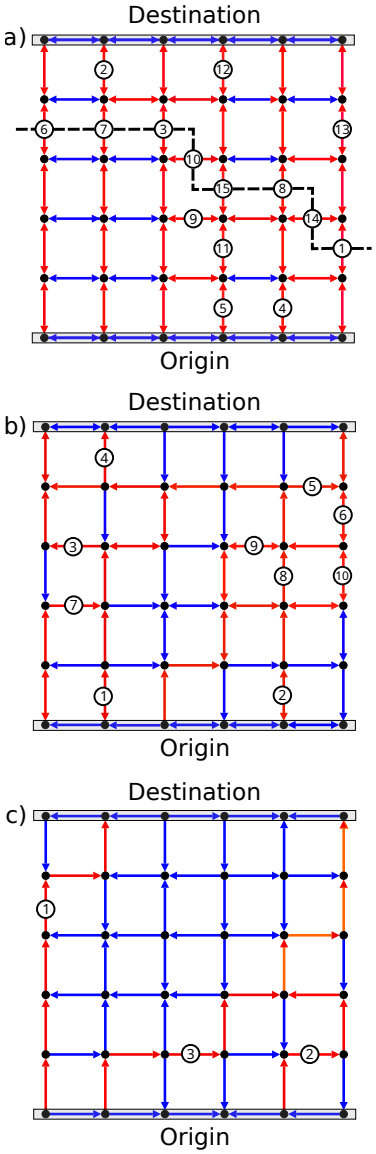

FIG. 1. Sequence of removed links during the OPC process for 6×6 square lattices under weak disorder in travelling times ($\beta = 0.002$) and different values of the fraction p of unidirectional links, namely, (a) $p = 0$, (b) $p = 0.4$, and (c) $p = 1$. Before the collapse of the system, all links in red were part of an optimal path, at least once, from the bottom (origin) to the top (destination) of the lattice. Those removed are indicated with white circles in the middle, numbered according to the OPC removal sequence, as explained in the main text. The number of removed links clearly decreases with p. The dashed line in (a) corresponds to the fracture backbone that is always present as a result of the OPC process applied to fully bidirectional networks ($p = 0$) [17].

lattice, while for $p = 1$ all links are unidirectional. Disorder is introduced by assigning the travelling times of unidirectional links according to a hyperbolic distribution $p(\tau_i) \propto 1/\tau_i$, truncated between $\tau_{max} = 1$ and $\tau_{min} = \exp(-\beta)$, where $\beta \geq 0$ is the parameter that controls the disorder. Note that, in general, each bidirectional link in the network have distinct travelling times associated to its two directions. Typical realizations of the OPC model for small networks generated with weak disorder are shown in Fig. 1. As previously observed [17], the set of OPC cracks generated in fully bidirectional networks ($p = 0$) always contains a contiguous subset that spans the entire system from left to right, regardless of the level of disorder. In the presence of any amount of unidirectional links ($p > 0$), however, the cracks do not necessarily form a contiguous fracture that divides the network into two pieces. Moreover, the larger the value o p, more rare is the occurrence of these spanning fractures.

Figure 2 shows the logarithmic dependence of the number of removed links N_r on the linear size of the lattice L, for lattices with sizes varying in the range $16 \leq L \leq 512$ and weak disorder in their distribution of travelling times ($\beta = 0.002$). For $p \neq 1$, the numerical results are consistent with $N_r \sim L^d$, where $d = 2$. This result suggests that, provided the lattice contains a non-zero fraction of bidirectional links, the set of all removed links is compact, as reported previously for regular lattices with only bidirectional links ($p = 0$) [17]. Nevertheless, the fraction of removed links is a monotonic decreasing function of p and so, the prefactor of the power-law dependence decreases also with p (see Fig. 1). Surprisingly, in the limiting case of a completely unidirectional lattice, $p = 1$, we find that $N_r \sim L^{D_f}$, with $D_f = 0.382 \pm 0.002$. Our results therefore indicate that the OPC set at this point belongs to a different universality class. Moreover, since $D_f < d$, the fraction of removed links for an infinite lattice (thermodynamic limit) is zero for $p = 1$.

The statistics of the OPC set generated under weak disorder suggests that its dimension does crossover from d, for $p > 1$, to D_f at $p = 1$. This crossover is analogous to what is observed at the theta point of polymer systems [25–27]. At high temperatures, the configurations of a polymer chain are well described by a self-avoiding random walk, as the only relevant interactions are excluded volume. However, at the theta-temperature, the attractive forces are no longer negligible, and the statistics are then different. Also, in ranked surfaces, when occupying links sequentially, but suppressing global connectivity, the fractal dimension of the set of links that are not occupied due to this constraint changes from 3/4 at the percolation threshold to 1.22 above it [28]. For the case of OPC, we consider the following crossover *Ansatz*:

$$N_r = L^D \mathcal{F}\left[(p - p_c)\, L^\theta\right], \qquad (1)$$

where θ is the crossover exponent, $\mathcal{F}[x] \sim x^\eta$ for $x \neq 0$ and equal to a nonzero constant at $x = 0$. The inset in Fig. 2 shows the data collapse obtained with this tricritical scaling for different lattice sizes and values of p, with $\theta = 0.753$. By fitting the power-law regime of the scaling function $\mathcal{F}$, we estimate $\eta = 2.15 \pm 0.03$. From

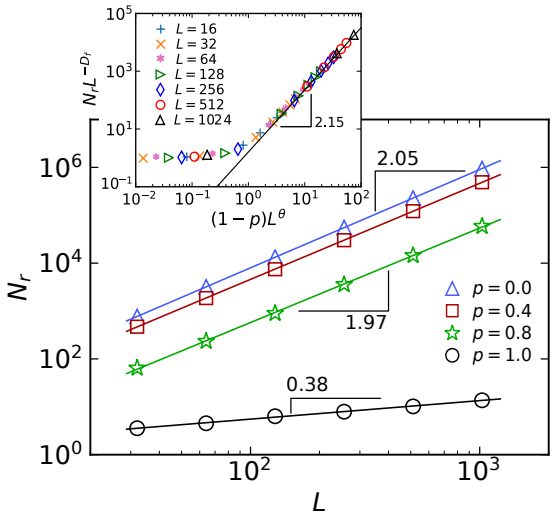

FIG. 2. Logarithmic dependence of the total number of removed links N_r on the linear size of the lattice L for different values of the fraction p of unidirectional links. The symbols correspond to averages over 100 thousand network realizations and weak disorder in their traveling times ($\beta = 0.002$). The results for $p = 0.4$ and 0.8 are consistent with the scaling, $N_r \sim L^2$, obtained for $p = 0$, namely, fully bidirectional lattices [17]. For a completely unidirectional lattice, $p = 1$, we find that $N_r \sim L^{D_f}$, with $D_f = 0.382 \pm 0.002$. The error bars are smaller than the symbols. The inset shows the tricritical crossover scaling and data collapse for the OPC model on regular lattices. The scaling function is given by Eq. (1), with $D_f = 0.38$ and $\theta = 0.753$. The solid line in the inset represents a power law with exponent 2.15.

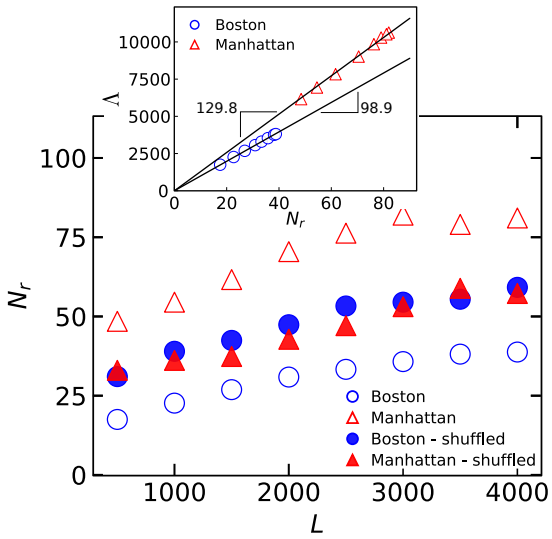

FIG. 3. Dependence of the total number of removed roads N_r on the origin-destination distance L (in meters) for downtown Boston and Manhattan (open symbols). Numerical results are averages over 2000 OD samples for each city. Also shown are the results of OPC simulations preserving the geometry of the road networks, but shuffling the values of t/ℓ among randomly chosen pairs of road segments (filled symbols). The inset shows the linear dependence, $\Lambda = aN_r$, with $a = 98.9 \pm 0.03$ and 129.8 ± 0.04 for Boston and Manhattan, respectively. In all cases, the error bars are smaller than the symbols.

the *Ansatz*, we expect that,

$$D_f + \eta\theta = d, \tag{2}$$

what is verified, within error bars. This behavior confirms that the universality class of OPC is robust and only breaks down for a fully unidirectional lattice ($p = 1$).

For the case of local travelling times with strong disorder, $\beta = 400$ (see Fig. S1 of the Supplemental Material), the OPC results for $p \neq 1$ are consistent with the behavior previously observed for fully bidirectional networks ($p = 0$), namely, $D_f = 1.22 \pm 0.01$ [17]. As in the weak disorder case, it is only for $p = 1$ that the finite-size scaling of the system becomes noticeably different, with $D_f = 0.002 \pm 0.004$. A rather small number of removed links is therefore sufficient to block a fully directed lattice subjected to strong disorder.

Next, we show that the OPC can be effectively used as a proxy for urban mobility. In general, the fraction of one-way roads changes from city to city. Here we apply the OPC method to two metropolitan areas in US, namely, Manhattan and downtown Boston, the latter being the top one in the rank of North America for average time waste in traffic [1]. For this purpose, we obtained the road network structures of both urban areas from OpenStreetMap [29]. Their corresponding average travelling times per road were downloaded from Directions API Google [30], specifically for November 21th of 2018 at 4:00 am. This off-peak data set has been chosen because, by construction, the travelling times should somehow reflect the freeway-state of the streets and avenues constituting a given urban mobility system. In order to assess the efficiency of these road networks to urban traffic, the OPC is numerically calculated for different pairs of origin-destination (OD) sites. Precisely, for each OPC realization, one site of the network is selected at random to be the center of a circle of radius L. A point on this circle is then randomly chosen and the closest road sites to the center and to this point are taken as the origin and destination, respectively, only if the distance between them is equal to L within a tolerance of 5%. Here, due to the fact that road segments composing the urban networks have different travelling times t as well as lengths ℓ, an optimal path is identified among all possible paths during the OPC process as the one with the minimum sum of t/ℓ over all its road segments.

OPC simulations have then been performed with 2000 OD realizations for Boston and Manhattan. One should note that the bidirectional links (two-way streets and avenues) are in fact composed of two unidirectional ones of contrary directions that can be removed independently during the OPC process. In Fig. 3, we show how the av-

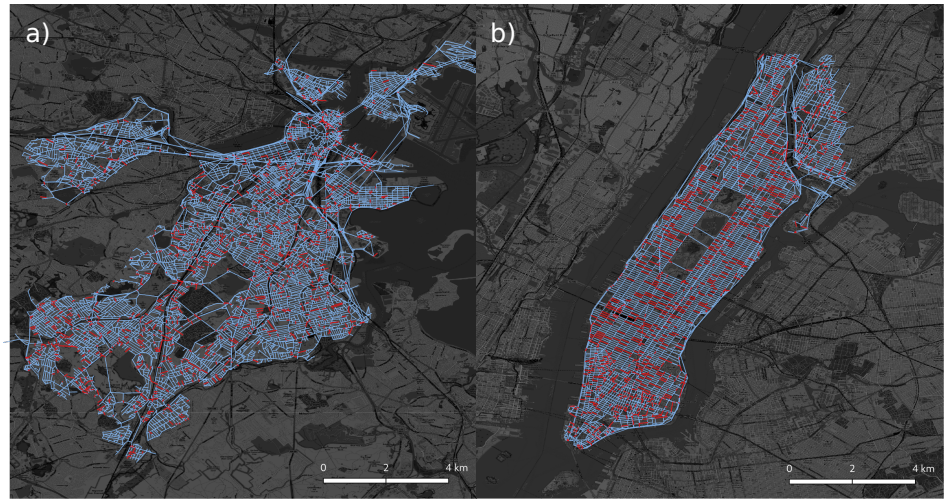

FIG. 4. Road maps for downtown Boston (left) and Manhattan (right). The thick red lines are the road segments that have been removed first. All other road segments are shown in blue. Only OPC samples performed with OD distances $L = 2000$ m have been considered.

erage number of removed sites N_r varies with the distance L for both urban areas. The smaller N_r is, less resilient is the road network. These results indicate that Boston is systematically much more vulnerable than Manhattan, regardless of the origin-destination distance L, what is consistent with their relative positions in the national rank of urban mobility. Moreover, the same behavior can be observed if, instead of N_r, we quantify the result of each OPC process in terms of the sum $\Lambda = \sum_{i=1}^{N_r} \lambda$, where λ is equal to the length ℓ of the removed road segment at iteration i. Interestingly, as shown in the inset of Fig. 3, these two measures are, in fact, linearly related $\langle \Lambda \rangle = aN_r$, with $a = 98.9\,\mathrm{m}$ and $129.8\,\mathrm{m}$ for Boston and Manhattan, respectively. For all practical purposes, this indicates the absence of statistical correlations in the OPC process of selecting λ from the distribution of segment lengths $P(\ell)$ of both road networks. The similarities between distributions $P(\ell)$ and $P(\lambda)$ for Boston and Manhattan are compatible with this argument (see Fig. S2 of Supplemental Material).

The modest differences in the distributions $P(t/\ell)$ obtained for Boston and Manhattan (see Fig. S3 of the Supplemental Material) are not compatible with such a striking discrepancy in their resilience. One therefore can only rely on the particular features of the intrinsic spatial correlations that should be present in these urban systems to justify their very distinct responses. In order to test for this hypothesis, we performed additional OPC simulations preserving the geometry of both networks, but shuffling the values of t/ℓ among randomly chosen pairs of road segments. The results presented in Fig. 3 are rather surprising and twofold. First, they show that the effect of suppressing the spatial correlations is to practically collapse the curves N_r against L of both cities to a single curve, therefore demonstrating the generality and comparative power of the OPC method for urban mobility. Second, the fact that the values of N_r systematically increase for Boston and decrease for Manhattan, as compared to the results using the real (non-shuffled) data sets, corroborates the ability of our approach to properly capture negative and positive effects of spatial correlations on urban mobility.

One question that naturally arises is how the OPC method can be used to enhance urban mobility. A possible answer is to prioritize rerouting and structural improvements based on the identification of those road segments that are more frequently appearing among the first removals in all OPC sequences. In Fig. 4 are the road maps for the two urban areas, where the highlighted road segments (thick and red) correspond to all those removed first, considering all OPC samples performed with OD distances $L = 2000$ m. For downtown Boston, we find that only a percentage of 5.4% of all road segments is removed, while 10.0% is the value for Manhattan. The cumulative dependence of the percentage of all first removals on the percentage of the most frequent ones is shown in Fig. S4 of the Supplemental Material. These results suggest that, as compared to Manhattan, a relatively small number of potential local changes in Boston might be very efficient in improving urban mobility. The fact that Manhattan is much more resilient should therefore increase the costs of improvements.

In summary, we proposed a proxy for resilience of urban mobility based on OPC. Our results with synthetic and real road networks suggest that their vulnerability to traffic congestion are strongly dependent on the level of disorder, fraction of unidirectional segments and intrinsic spatial correlations. These observations have practical implications in the design and restructuring for improved urban mobility. We conclude that OPC is a gen-

eral and powerful method to access urban mobility, and gives practical insight that can effectively help identifying and mitigating vulnerabilities of real road networks.

We acknowledge financial support from the Brazilian agencies CNPq, CAPES and FUNCAP, and from the Portuguese Foundation for Science and Technology (FCT) under Contracts no. UIDB/00618/2020 and UIDP/00618/2020.

* soares@fisica.ufc.br

[1] T. Reed and J. Kidd, *INRIX Global Traffic Scorecard 2018*, Tech. Rep. (IRIX Research, United States, 2018).
[2] M. Sweet, Urban Studies **51**, 2088 (2014).
[3] R. Louf and M. Barthelemy, Sci. Rep. **4**, 1 (2014).
[4] S. Colak, A. Lima, and M. C. González, Nat. Commun. **7**, 10793 (2016).
[5] A. Solé-Ribalta, S. Gómez, and A. Arenas, Networks Spat. Econ. **18**, 33 (2018).
[6] H. Barbosa, M. Barthelemy, G. Ghoshal, C. R. James, M. Lenormand, T. Louail, R. Menezes, J. J. Ramasco, F. Simini, and M. Tomasini, Phys. Rep. **734**, 1 (2018).
[7] M. Barthelemy, Nature Reviews Physics **1**, 406 (2019).
[8] D. Li, B. Fu, Y. Wang, G. Lu, Y. Berezin, H. E. Stanley, and S. Havlin, Proc. Natl. Acad. Sci. U. S. A. **112**, 669 (2015).
[9] M. C. González, C. A. Hidalgo, and A.-L. Barabási, Nature **453**, 779 (2008).
[10] L. E. Olmos, S. Çolak, S. Shafiei, M. Saberi, and M. C. González, Proc. Natl. Acad. Sci. U. S. A. **115**, 12654 (2018).
[11] G. Zeng, D. Li, S. Guo, L. Gao, Z. Gao, H. Eugene Stanley, and S. Havlin, Proc. Natl. Acad. Sci. U. S. A. **116**, 23 (2019).
[12] S. Zhu and D. Levinson, PLoS One **10**, e0134322 (2015).
[13] A. Lima, R. Stanojevic, D. Papagiannaki, P. Rodriguez, and M. C. Gonzalez, J. R. Soc. Interface **13** (2016).
[14] L. Zhang, G. Zeng, D. Li, H. J. Huang, H. Eugene Stanley, and S. Havlin, Proc. Natl. Acad. Sci. U. S. A. **116**, 8673 (2019).
[15] P. Wang, T. Hunter, A. M. Bayen, K. Schechtner, and M. C. González, Sci. Rep. **2**, 1001 (2012).
[16] S. Guo, D. Zhou, J. Fan, Q. Tong, T. Zhu, W. Lv, D. Li, and S. Havlin, EPJ Data Sci. **8**, 28 (2019).
[17] J. S. Andrade Jr, E. A. Oliveira, A. A. Moreira, and H. J. Herrmann, Phys. Rev. Lett. **103**, 225503 (2009).
[18] E. A. Oliveira, K. J. Schrenk, N. A. M. Araújo, H. J. Herrmann, and J. S. Andrade, Phys. Rev. E **83**, 046113 (2011).
[19] E. W. Dijkstra, Numer. Math. **1**, 269 (1959).
[20] M. Cieplak, A. Maritan, and J. R. Banavar, Phys. Rev. Lett. **72**, 2320 (1994).
[21] M. Cieplak, A. Maritan, and J. R. Banavar, Phys. Rev. Lett. **76**, 3754 (1996).
[22] M. Porto, S. Havlin, S. Schwarzer, and A. Bunde, Phys. Rev. Lett. **79**, 4060 (1997).
[23] M. Porto, N. Schwartz, S. Havlin, and A. Bunde, Phys. Rev. E **60**, R2448 (1999).
[24] R. Dobrin and P. M. Duxbury, Phys. Rev. Lett. **86**, 5076 (2001).
[25] P.-G. de Gennes, *Scaling concepts in polymer physics* (Cornell University Press, Ithaca, New York, 1979).
[26] I. Chang and A. Aharony, J. Phys. I **1**, 313 (1991).
[27] P. H. Poole, A. Coniglio, N. Jan, and H. E. Stanley, Phys. Rev. B **39**, 495 (1989).
[28] K. J. Schrenk, N. A. M. Araújo, J. S. Andrade Jr, and H. J. Herrmann, Sci. Rep. **2**, 348 (2012).
[29] OpenStreetMap contributors, "Planet dump retrieved from https://planet.osm.org," `https://www.openstreetmap.org` (2019).
[30] Google, "Google Directions API," `https://developers.google.com/maps/documentation/directions/start` (2019).